Fabrication and physical properties of radio frequency sputtered $Cd_{1-x}Mn_xS$ thin films

C. T. Tsai, S. H. Chen, and D. S. Chuu*
Institute of Electrophysics, National Chiao Tung University, Hsinchu, Taiwan, Republic of China

W. C. Chou
Department of Physics, Chung Yuan Christian University, Chung Li, Taiwan, Republic of China
(Received 9 February 1996; revised manuscript received 27 May 1996)

Highly oriented $Cd_{1-x}Mn_xS$ thin films with a wurtzite structure were grown by the radio-frequency sputtering technique. The grain size of the $Cd_{1-x}Mn_xS$ thin films was found to decrease with an increase in the Mn concentration x. Moreover, the lattice softening effect due to the quantum size effect, the band-bowing phenomena accounted for by the band-gap correction arising from the chemical disorder, and the exchange interaction between the band carrier and the d electron of the magnetic Mn ions have been investigated. [S0163-1829(96)01140-X]

I. INTRODUCTION

Advances in epitaxy growth have opened additional avenues for studies in semiconductor physics. A number of physical phenomena were discovered when the physical dimensions of semiconductors were tailored from bulk to two-dimensional microstructures,[1] one-dimensional microstructures,[2] or even to zero-dimensional quantum dots.[3] Among the quantum structures which have been studied, diluted magnetic semiconductor (DMS)-based structures[4] have distinguished themselves from the others due to the inherited giant magnetic-field-induced band splitting and the interesting magnetism. The magnetic tuning of the band alignment in a quantum well,[5] a spin superlattice,[6] the polaron in a type-II quantum well,[7] magnetic ordering in two dimensions,[8] and many other exciting physical phenomena[9] have been observed in DMS-based microstructures. To date, thousands of papers on DMS (Ref. 9) have been published. However, there remain several kinds of DMS's which are not well explored. Among them, $Cd_{1-x}Mn_xS$-based microstructures have been the least investigated.

In this study, the radio-frequency (rf) sputtering technique is used to grow $Cd_{1-x}Mn_xS$ thin films with a thickness of approximately 400 nm. The purpose is to investigate the lattice softening of the longitudinal optical (LO) phonon in the $Cd_{1-x}Mn_xS$ thin films. As was reported recently by the present researchers,[10] lattice softening in a LO phonon observed in CdS thin films grown by pulsed laser evaporation is attributed to the size quantization of the grain size and to low-dimensional thin-film structures. It is, therefore, suspected that the lattice vibration of the rf-sputtered $Cd_{1-x}Mn_xS$ thin films will be quite different from that of the bulk $Cd_{1-x}Mn_xS$ crystals due to the quantum size effect. In addition to phonon Raman work, the present researchers have implemented the transmission experiments to measure the band gap of $Cd_{1-x}Mn_xS$ thin films for a study of the band-bowing effects. It was found that the band-bowing effects of $Cd_{1-x}Mn_xS$ thin films can be explained by band-gap corrections caused by the chemical disorder and the exchange interaction between the carrier and the magnetic Mn ions.

II. EXPERIMENTAL PROCEDURE

$Cd_{1-x}Mn_xS$ thin films were fabricated in a rf sputtering system consisting mainly of a dual planar magnetron sputter gun (US' GUN II, Model SU-500V), a rf generator (US' GUN II, Model SU-600RF), and an automatic tuning network (US' GUN II. SU-600ATN). A rotary van pump (Balzers DUO 016B) was used in conjunction with a turbomolecular pump (Balzers, TPH 190) to evacuate the growth chamber to a pressure of about 10^{-7} torr. As the lowest pressure was reached, a high-purity (99.999) argon gas which was controlled precisely and stabilized by a gas dosing valve (Balzers UDV 035) was introduced to maintain the chamber pressure at 5×10^{-2} torr throughout the entire whole growth process.

The CdS and MnS powders were pressed into a circular plate 2 in. in diameter as the sputtered targets for the dual sputter guns. Either Corning glass slices or (100) p-type silicon wafers were used as the substrate. The distance between the substrate and the target was 5 cm. To ensure a good quality of $Cd_{1-x}Mn_xS$ thin films, a 15-min presputtering cleaning was performed. During the sputtering the substrates were heated by two independent cumulative processes, one being the inherent heating from the plasma on the sample, the other being performed by the extra heating from the sample holder using a tungsten halogen lamp. A chromel-alemmal thermocouple was attached to the surface of an additional dump substrate to monitor the substrate temperature. For every run, the substrate was heated to 300 °C for 2 h so that the thermal cleaning could be accomplished before the deposition of the $Cd_{1-x}Mn_xS$ thin films. The substrate temperature was then lowered down to 200 °C to begin the sputtering process, with the output power to the rf sputtering guns varying from 40 to 120 W for different Mn concentrations. A rapid thermal annealing process with a ramping rate of 100 °C/s and an annealing temperature of 400–700 °C for 15 to 120 s was implemented after the deposition of the films. To cool the sample to room temperature, rates of 100–250 °C/s were tried. After many trials it was found that the optimum annealing temperature is 600 °C for a time period of 60 s. To study the crystallinity and surface morphology,

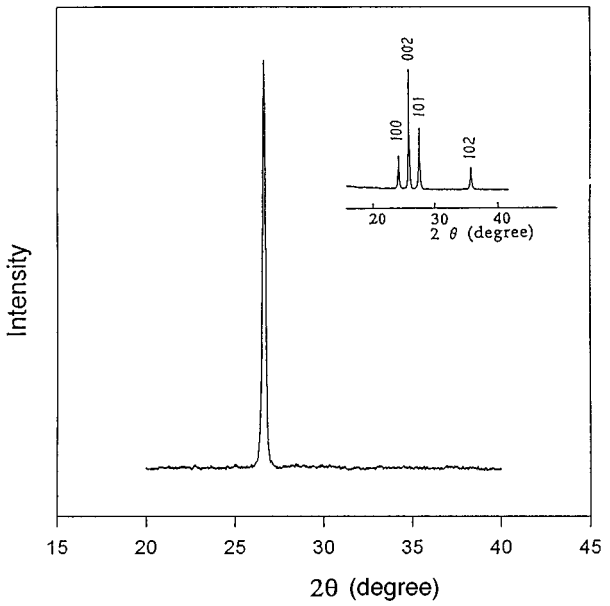

FIG. 1. The XRD spectrum of $Cd_{1-x}Mn_xS$ films on a *p*-type (100) silicon wafer with $x=0.139$. The upper right side of the figure is the XRD pattern of CdS powder.

x-ray diffraction (XRD) and scanning electron microscopy (SEM) with a resolution of 15 Å were used. The thickness of the highly oriented films was measured by an ellipsometer with a resolution of 10 Å. The molar concentration of the constituent elements of the $Cd_{1-x}Mn_xS$ thin films was determined by an energy-dispersive analysis of x-ray (EDAX) measurement. Lattice vibration by Raman spectroscopy was also studied. An argon 4880 Å line with a power of about 100 mW was used as the excitation for the Raman spectra. The spectra were recorded in 45° reflection geometry with samples being placed under the micrometer stage of a triple-grating spectrograph (SPEX 1877C) equipped with a liquid-nitrogen-cooled charge coupled device (CCD) detector array (Photometrics CCD200). For the absorption experiments the samples were placed on the cold finger of a closed cycle refrigerator with the temperature varying from 10 K to room temperature for the study of the band-gap dependence on the temperature.

III. RESULTS AND DISCUSSIONS

The structure and crystallinity of the $Cd_{1-x}Mn_xS$ thin films were analyzed by the XRD with a Cu $K\alpha$ source (wavelength 1.54 Å). In Fig. 1 the XRD spectrum from the $Cd_{1-x}Mn_xS$ thin films grown on a *p*-type silicon wafer with a Mn concentration $x=0.139$ is shown. On the upper right-hand side of Fig. 1, the results from the CdS powder are shown for comparison. X-ray diffraction from the (100), (002), (101), and (102) surfaces was observed for the CdS powder. While in the case of the $Cd_{1-x}Mn_xS$ thin films only sharp diffraction from the (002) surface was observed, this result indicates that the $Cd_{1-x}Mn_xS$ thin films oriented highly in the (002) direction exhibit a favorable crystalline structure. Furthermore, an increase in the Bragg angle was found for the $Cd_{1-x}Mn_xS$ thin films. The lattice constant *c* along the *c* axis of the $Cd_{1-x}Mn_xS$ thin films was

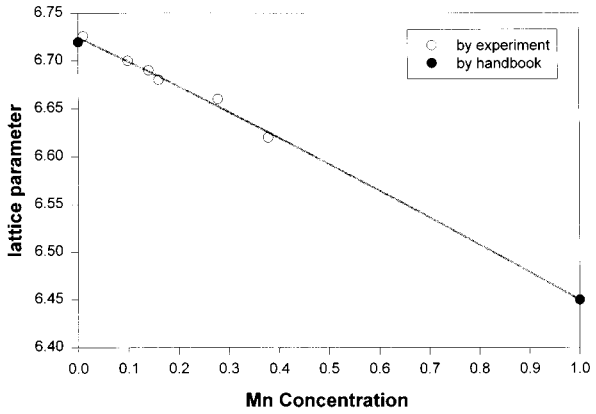

FIG. 2. The lattice parameters of $Cd_{1-x}Mn_xS$ thin films in the *c*-axis direction varied with Mn concentration.

obtained using the equations $2d\sin\theta=n\lambda$ and $d=c/\{h^2(a/c)^2+k^2(a/c)^2+l^2\}^{1/2}$, where $(hkl)=(002)$. In Fig. 2 the lattice constant *c* measured by the XRD for the $Cd_{1-x}Mn_xS$ thin films is plotted versus the Mn concentration determined by the EDAX results. A linear behavior which follows Vegard's law was found. The lattice constant decreases as the Mn concentration is increased due to the smaller atomic size of Mn than that of Cd. Note that for strained thin films, one might expect lattice distortion due to the stress between the substrate and the thin film. Therefore, a slight deviation from the line which describes the dependence of the lattice constant on the Mn concentration of the bulk crystals might be observed. However, Fig. 2 shows that the linear dependence of the lattice constant on Mn concentration for the experimental film is consistent with that of the bulk crystal within the experimental error. Since the thicknesses of the experimental $Cd_{1-x}Mn_xS$ thin films were all about 400 nm, the results indicated that the strain between the substrates and thin films was released for the films having a thickness of ~400 nm. Hence, for all $Cd_{1-x}Mn_xS$ thin films used in this study, the dependence of the lattice constant and Mn concentration follows that of the bulk crystals.

The surface morphology of the $Cd_{1-x}Mn_xS$ thin films investigated by SEM is shown in Fig. 3 for Mn concentrations of $x=0.01$, 0.098, 0.278, and 0.378. As shown in Fig. 3, the grain size of the $Cd_{1-x}Mn_xS$ thin films decreases as *x* increases. This result is corroborated by the XRD work. As the Mn concentration is increased, the diffraction peak of the XRD spectra becomes broader due to a reduction in the grain size. It is recalled that the perfect infinite crystal should have an XRD peak with a δ-function shape. Note that the other reason for broadening in the XRD spectra might be the increase in the chemical disorder as *x* is increased. The reason that the grain size decreases as *x* increases can be understood as follows. A stable crystal structure of CdS (wurtzite) differs from that of MnS (rocksalt). As the composition *x* of the $(CdS)_{1-x}(MnS)_x$ solid solution increases, internal strain arises, and the crystal structure of the CdMnS solid solution becomes unstable. In order to stabilize the crystal structure, the grain size is reduced to release the strain as the Mn concentration becomes larger.

In this study, band-bowing phenomena were investigated by transmission spectroscopy. In Fig. 4(a) variation in en-

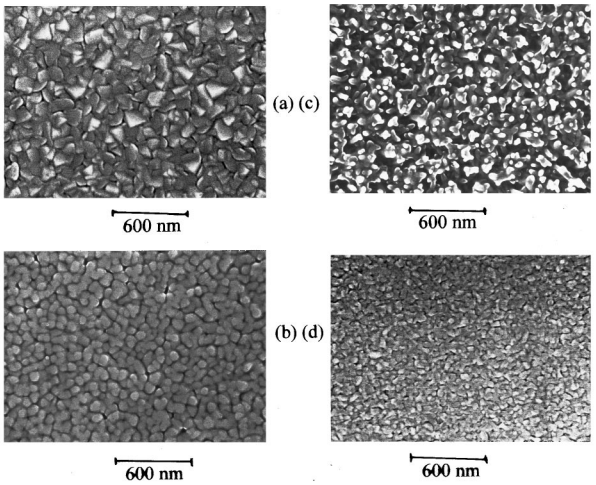

FIG. 3. SEM photographs of $Cd_{1-x}Mn_xS$ thin films with variations of Mn concentration were (a) $x=0.01$, (b) $x=0.098$, (c) $x=0.278$, and (d) $x=0.378$, respectively.

ergy gap versus x at 297 K (black circle), along with the results obtained by Ikeda, Itoh, and Sato[11] (triangulars) for the bulk $Cd_{1-x}Mn_xS$ crystals at 298 K is shown. The band gap of the CdS thin film, having a small grain size of roughly 150–200 Å, is larger than that of the bulk CdS crystal by several meV due to the quantum size effect.[10] In Fig. 4(b) the dependence of the energy gap on x at 10 K is shown. One can note from Figs. 4(a) and 4(b) that the band gap increases as the temperature decreases. The band-bowing effect, the band gap initially decreasing at a low value of x then increasing with an increase in the Mn concentration x, can be observed for both the bulk $Cd_{1-x}Mn_xS$ crystals and the $Cd_{1-x}Mn_xS$ thin films in Fig. 4(a) and (b). However, the Mn concentration x, where the minimum of the band gap occurs, and the curvature of the band gap and x relationship curve are different for thin films and the bulk. For the bulk crystal the minimum occurs at $x=0.04$; whereas, in the case of a $Cd_{1-x}Mn_xS$ thin film, the minimum is around $x=0.065$. To understand this discrepancy, the origin of the band bowing effect for ternary compounds should be studied.

The band-bowing phenomena found in the DMS bulk crystal were attributed to the correction in the exchange interaction with the conduction and valence band.[12] The band-bowing effect was also observed in the nonmagnetic semiconductors.[13–15] However, in the case of nonmagnetic semiconductors, chemical disorder[14] was recognized as the only source for the band bending, because there are no magnetic ions like Mn, Fe, Co, or Cr existing in the nonmagnetic semiconductors to cause the exchange interaction between the carrier and the magnetic ions. Recently,[16] the present researchers stated that the effect of both the exchange interaction and the chemical disorder on the conduction and valence bands should be considered explanations for the band-bowing effect found in $Cd_{1-x}Fe_xS$ bulk crystals.

The variation in the energy gap on x for the ternary compounds $A_{1-x}B_xC$ can be written as

$$E_g(x,T)=E_0(T)+\mathbf{a}x-\mathbf{b}x(1-x)+E_M(x,T), \qquad (1)$$

where $E_0(T)$ is the band gap of the binary compound AC at temperature T. The parameter **a**, describing the linear variation of the band gap on x, is the energy difference between the band gaps of AC and BC. The parameter **b** is another parameter representing the strength of the chemical disorder. $E_M(x,T)$ is a correction caused by the exchange interaction [12,16]. Without the last term, Eq. (1) describes the band-bowing phenomena of a nonmagnetic semiconductor arising from the chemical disorder existing in the ternary compound $A_{1-x}B_xC$. The values of **b** are 0.58 eV (for the $Z_{1,2}$ exciton peaks at 80 K), 0.18 eV, and 1.4 eV for $Ag_{1-x}Cu_xI$,[13]

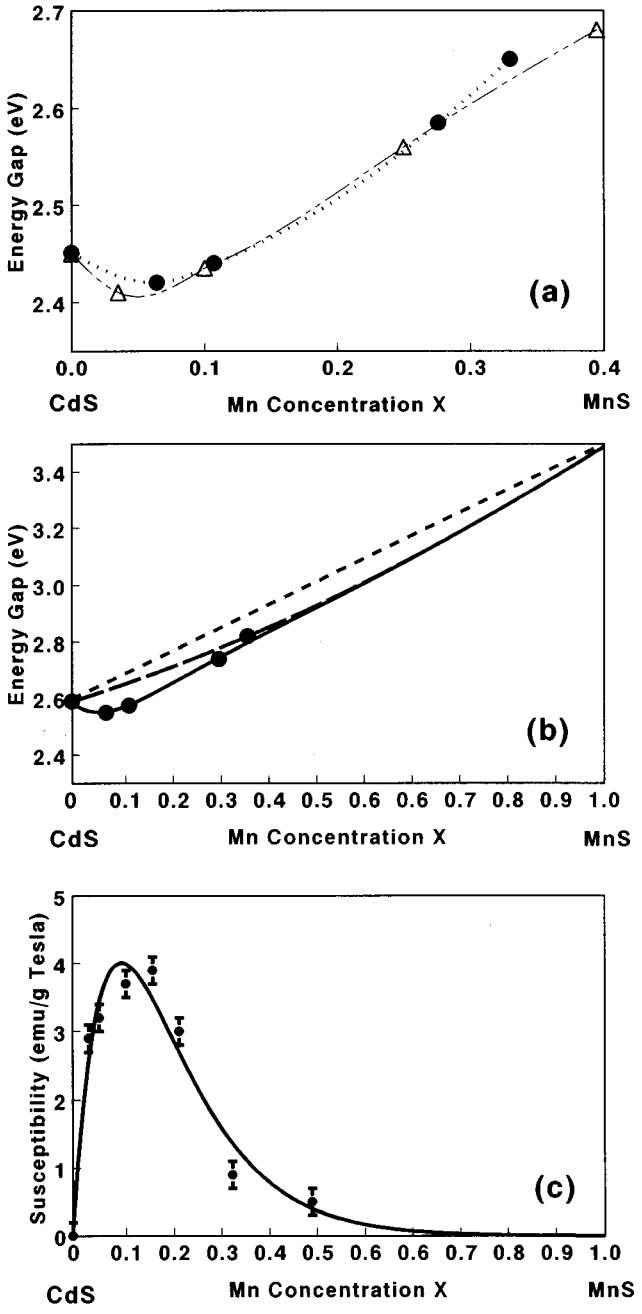

FIG. 4. (a) Variation of the energy gap of $Cd_{1-x}Mn_xS$ with Mn concentration by our samples at 297 K (black circles) and the results of Ikeda, Itoh, and Sato at 298 K (triangulars). (b) Variation of the energy gap of $Cd_{1-x}Mn_xS$ with Mn concentration by our samples at 10 K. The solid line is the fitted curve. (c) Experimental data of the susceptibility varied with Mn concentration as obtained by Ref. 17.

$Ga_{1-x}As_xP$,[14] and $ZnSe_xTe_{1-x}$,[15] respectively. A larger **b** indicates a stronger deviation from the linear variation in the band gap between the two binary compounds. For nonmagnetic semiconductors the maximum deviation from the linear relation occurs near $x=0.5$. In order to describe the band-bowing effect which happens at values of x much smaller than 0.5, the last term in Eq. (1) must be included. The energy correction $E_M(x,T)$ for the band gap in cubic structure semiconductors due to the exchange interaction can be obtained by the following perturbative calculation:[12]

$$E_M(x,T)=-[\Omega_o]^2\frac{k_BT}{(g\mu_B)^2}\frac{p_o}{h^2}\chi[3m_e\alpha^2+(m_{\rm hh}+\tfrac{2}{3}m_{\rm lh})\beta^2] \tag{2}$$

where Ω_o is the unit-cell volume, p_o is a parameter characterizing the range of the exchange interaction in k space, k_B is the Boltzmann constant, g is the g factor, μ_B is the Bohr magneton, and χ is the susceptibility of the crystals obtained by the magnetization measurement. The electron, heavy hole (hh), and light hole (lh) effective masses are represented by m_e, $m_{\rm hh}$, and $m_{\rm lh}$, respectively. The parameters α and β are the exchange constants which correspond to the conduction and valence bands, respectively, while, for hexagonal structures, the correction for the band gap is written as[16]

$$E_M(x,T)=-(E_e-E_A). \tag{3}$$

The correction E_e for the conduction band (Γ_7) is given by

$$E_e=m_ep_o[\alpha\Omega_o]^2\frac{k_BT}{(gh\mu_B)^2}(\chi_\parallel+2\chi_\perp) \tag{4}$$

and the correction for the heavy-hole band (Γ_9) is

$$\begin{aligned}E_A=&m_Ap_o[\Omega_o\beta]^2\frac{k_BT}{(gh\mu_B)^2}(\chi_\parallel+2(1-q^2)\frac{m_B}{m_A}\chi_\perp\\&\times\left(1-\frac{\sqrt{2m_B(E_B-E_A)}}{\hbar p_o}\right)\arctan\left(\frac{\hbar p_o}{\sqrt{2m_B(E_B-E_A)}}\right)\\&+2q^2\frac{m_c}{m_A}\chi_\perp\left(1-\frac{\sqrt{2m_c(E_C-E_A)}}{\hbar p_o}\right)\\&\times\arctan\left(\frac{\hbar p_o}{\sqrt{2m_c(E_C-E_A)}}\right),\end{aligned} \tag{5}$$

where m_A, m_B, and m_C are the hole-effective masses corresponding to the A, B, and C excitons. The Greek symbol $\chi_\parallel$ ($\chi_\perp$) represents the magnetic susceptibility for a magnetic field parallel (perpendicular) to the crystal hexagonal axis. The parameter q^2 is the wave-function mixing coefficient for a hexagonal crystal, and is given by[16]

$$q^2=\frac{1}{2}\left(1-\frac{\Delta_1-\Delta_2}{\sqrt{(\Delta_1-\Delta_2)^2+8\Delta_3^2}}\right), \tag{6}$$

Δ_1, Δ_2, and Δ_3 are the conventional crystal-field and spin-orbit parameters. In the case of $Zn_{1-x}Mn_xSe$,[12] the effect of the chemical disorder was neglected to account for the band bowing. By considering only the exchange interaction correction, the dependence of the susceptibility on the Mn concentration explains the band-bowing effect. The band bowing-effect in the $Cd_{1-x}Mn_xS$ thin films is similar to the case of the $Zn_{1-x}Mn_xSe$ crystals. By using the results obtained by Chen *et al.*[17] [Fig. 4(c)] for the dependence of the susceptibility on x which assumes $\chi_\parallel$ to be equal to $\chi_\perp$, the band gap versus x data for the $Cd_{1-x}Mn_xS$ thin films can be fitted as shown by the solid lines in Fig. 4(b) at 10 K. To accommodate the data, a simplified equation is used:

$$E_g(x,T)=E_0(T)+\mathbf{a}x-\mathbf{b}x(1-x)+c\chi T. \tag{7}$$

In this way the complex form of $E_M(x,T)$ can be represented by the fitting parameter $c'=cT$ and the experimental data χ as presented in Fig. 4(c). The fitting parameter c' is a function of all the parameters, like the effective mass, the crystal-field parameter, and the exchange constant, in Eqs. (4)–(6). In Fig. 4(b) the smaller dashed lines were obtained by setting b and c to zero, assuming the gap in the MnS is 3.5 eV. For the longer dashed line in Fig. 4(b), $\mathbf{a}=0.9$ eV, $\mathbf{b}=0.3$ eV, and $c'=0$ were used. Then both the chemical disorder and the correction due to the exchange interaction by using $\mathbf{a}=0.9$ eV, $\mathbf{b}=0.3$ eV, and $c'=-0.02$ eV g T/emu, as shown by the solid line in Fig. 4(b), were considered. The solid lines fit the experimental data in a reasonable way. It was found that the parameter **b** obtained for the $Cd_{1-x}Mn_xS$ thin films is smaller than that of the nonmagnetic semiconductors.[13–15] It is noted that parameters[18] like the effective mass, exchange constant, and crystal-field parameter which were absorbed in c' might vary with x. Moreover, it is realized that the grain size of the $Cd_{1-x}Mn_xS$ thin films is at least several hundred Å and also depends on the Mn concentration. The size of the microstructure might have an effect on the exchange interaction constants[19] α and β in the equations; however, it is undoubted that both the chemical disorder and the exchange interaction should be used to account for the band-bowing effect. In addition to the transmission experiment on the thin films, the phonon Raman spectra on the $Cd_{1-x}Mn_xS$ thin films, as shown in Fig. 5 have been taken. The energy of the LO phonon of the CdS thin films is 300 cm^{-1} and is smaller than that of the bulk CdS crystals. The decrease in the LO-phonon energy was attributed to the lattice softening[10] of the CdS thin films. As some of the Cd atoms are substituted for by Mn atoms, the LO-phonon energy exhibits a blueshift. At $x=0.159$, a weak shoulder was developed at the higher-energy side of the LO-phonon peak. As x was further increased to 0.378, two peaks were clearly observed. The LO-phonon energies from the $Cd_{1-x}Mn_xS$ thin films were plotted as a function of the Mn concentration x in Fig. 6, along with the results obtained by Suh *et al.*[20] (circles) for $Cd_{1-x}Mn_xS$ bulk crystals. The LO-phonon frequencies of the bulk crystals seem to be insensitive to the Mn concentration x, while for thin films the LO phonon splits into two peaks (triangulars), which are assigned like the MnS-like phonons when x is increased. As a result, the two-mode model seems to describe the Raman shift versus x plot of the $Cd_{1-x}Mn_xS$ thin films more appropriately than the intermediate mode behavior used to explain the phonon Raman work for the $Cd_{1-x}Mn_xS$ crystals by Suh *et al.* One might attribute the splitting of the LO phonon of the

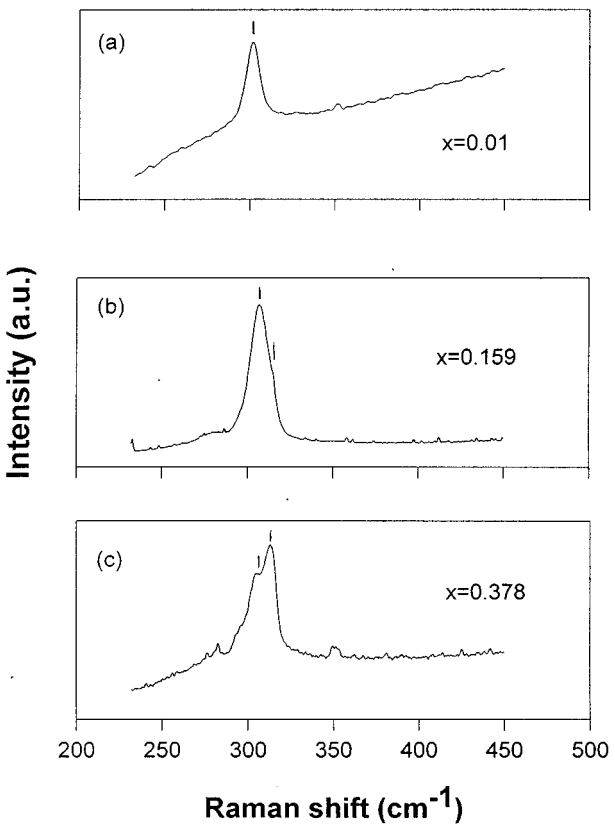

FIG. 5. Raman spectra of CdMnS thin films at 10 K with Mn concentration were (a) $x=0.01$, (b) $x=0.159$, and (c) $x=0.378$, respectively.

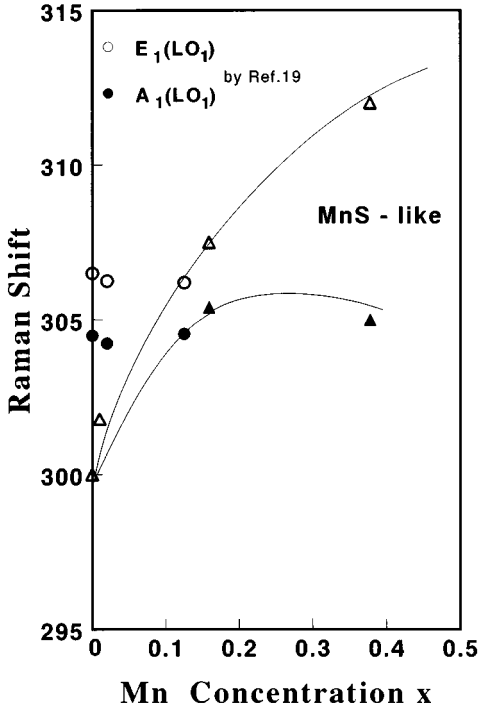

FIG. 6. The LO-phonon energies from the $Cd_{1-x}Mn_xS$ thin films varied as a function of the Mn concentration (triangulars). The results for the $Cd_{1-x}Mn_xS$ bulk crystals obtained by Ref. 20 (circles) was also presented for comparison.

$Cd_{1-x}Mn_xS$ thin films as being due to the strain between the substrate and the thin film. However, the thickness of the tested samples is approximately 400 nm. With such a thickness the strain between the substrate and the thin film is released; therefore, there is no need to consider the lattice strain in the substrate to interpret the observed Raman shift. To investigate the strain effect on the Raman shift, one needs to grow thinner films; however, the thinner the film, the worse the sample quality.

IV. CONCLUSIONS

Highly oriented $Cd_{1-x}Mn_xS$ thin films with a wurtzite structure were fabricated by using the rf sputtering technique with rapid thermal annealing. It was found that the grain size decreased as the Mn concentration increased. In addition, it was emphasized that physical properties, such as the band-bowing effects and the lattice vibration, of the thin films are very different from those of the bulk crystals. A detailed theoretical model is yet to be developed for the explanation of the discrepancy between the two types of $Cd_{1-x}Mn_xS$ structures.

ACKNOWLEDGMENTS

This study was partially supported by the National Science Council of Taiwan, the Republic of China. The authors also wish to express appreciation to Dr. Cheryl J. Rutledge for technical assistance.

*Author to whom correspondence should be addressed.

[1] S. Huant, S. P. Najda, and B. Etienne, Phys. Rev. Lett. **65**, 1486 (1990); M. R. Freeman, D. D. Awschalom, J. M. Hong, and L. L. Chang, *ibid.* **64**, 2430 (1990).

[2] M. Kohl, D. Heitmann, P. Grambow, and K. Ploog, Phys. Rev. Lett. **63**, 2124 (1989); S. Ueno, Y. Miyake, and M. Asada, Jpn. J. Appl. Phys. **31**, 286 (1992); I. Grodnensky, D. Heitmann, K. v. Klitzing, K. Ploog, A. Rudenko, and A. Kamaev, Phys. Rev. B **49**, 10 778 (1994).

[3] B. Meurer, D. Heitmann, and K. Ploog, Phys. Rev. Lett. **68**, 1371 (1992); M. A. Reed, J. N. Randall, R. J. Aggarwal, R. J. Matyi, T. M. Moore, and A. E. Wetsel, *ibid.* **60**, 535 (1988).

[4] J. K. Furdyna, J. Appl. Phys. **64**, R29 (1988).

[5] X. Liu, A. Petrou, J. Warnock, B. T. Jonker, G. A. Prinz, and J. J. Krebs, Phys. Rev. Lett. **63**, 2280 (1989).

[6] W. C. Chou, A. Petrou, J. Warnock, and B. T. Jonker, Phys. Rev. Lett. **67**, 3820 (1991).

[7] D. D. Awschalom, M. R. Freemann, N. Samarth, H. Luo, and J. K. Furdyna, Phys. Rev. Lett. **66**, 1212 (1991).

[8] N. Samarth, P. Klosowski, H. Luo, T. M. Giebultowicz, J. K. Furdyna, J. J. Rhyne, B. E. Larson, and N. Otsuka, Phys. Rev. B **44**, 4701 (1991).

[9] J. Furdyna and J. Kossut, *Diluted Magnetic Semiconductors*, Semiconductors and Semimetals Vol. 25 (Academic, New York, 1988); *Semimagnetic Semiconductors and Diluted Magnetic Semiconductors*, edited by M. Averous and M. Balkanski (Ple-

num, New York, 1991); *Diluted Magnetic Semiconductors*, edited by J. Mukesh (World Scientific, Singapore, 1991).
[10] D. S. Chuu, and C. M. Dai, Phys. Rev. B **45**, 11 805 (1992); C. T. Tsai, D. S. Chuu, G. L. Chen, and S. L. Yang, J. Appl. Phys. **79**, 15 (1996); D. S. Chuu, C. M. Dai, W. F. Hsieh, and C. T. Tsai, *ibid.* **69**, 8402 (1991).
[11] M. Ikeda, K. Itoh, and H. Sato, J. Phys. Soc. Jpn. **25**, 455 (1968).
[12] R. B. Bylsma, W. M. Becker, J. Kossut, U. Debska, and D. Yoder-Short, Phys. Rev. B **33**, 8207 (1986).
[13] M. Cardona, Phys. Rev. **129**, 69 (1963).
[14] A. G. Thompson and J. C. Woolley, Can. J. Phys. **45**, 255 (1967); A. Zunger and J. E. Jaffe, Phys. Rev. Lett. **51**, 662 (1983).
[15] B. Freytag, P. Pavone, U. Rossler, K. Wolf, S. Lankes, G. Schotz, A. Naumov, S. Jilka, H. Stanzl, and W. Gebhardt, Solid State Commun. **94**, 103 (1995).
[16] W. C. Chou, S. S. Kuo, F. R. Chen, A. Twardowski, J. Tworzydlo, and Y. F. Chen, Phys. Status Solidi B **193**, 125 (1996).
[17] C. Chen, M. Qu, W. Hu, X. Zhang, F. Lin, H. Hu, K. Ma, and W. Giriat, J. Appl. Phys. **69**, 6114 (1991).
[18] A. Twardowski, K. Chern-Yu, F. R. Chen, S. S. Kuo, C. S. Ro, K. C. Chiu, W. C. Chou, S. L. Yang, D. S. Chuu, and Y. F. Chen, Phys. Status Solidi (B) **181**, 439 (1994).
[19] T. Stirner, W. E. Hagston, and P. Harrison, Phys. Rev. B **52**, 5519 (1995).
[20] E. Suh, A. K. Arora, A. K. Ramdas, and S. Rodriguez, Phys. Rev. B **45**, 3360 (1992).